Search for the Blazhko effect in field RR Lyrae stars using LINEAR and ZTF light curves

Ema Donev[1] and Željko Ivezić[2]

[1] XV. Gymnasium (MIOC), Jordanovac 8, 10000, Zagreb, Croatia, e-mail: emadonev@icloud.com
[2] Department of Astronomy and the DiRAC Institute, University of Washington, 3910 15th Avenue NE, Seattle, WA, USA e-mail: ivezic@uw.edu

October 2024

ABSTRACT

We analyzed the incidence and properties of RR Lyrae stars that show evidence for amplitude and phase modulation (the so-called Blazhko Effect) in a sample of ~3,000 stars with LINEAR and ZTF light curve data. A preliminary subsample of about ~530 stars was algorithmically pre-selected using various data quality and light curve statistics, and then 228 stars were confirmed visually as displaying the Blazhko effect. This sample places a lower limit of 7% for the incidence of the Blazhko Effect in field RR Lyrae stars. Although close to 8,000 Blazhko stars were discovered or confirmed in the Galactic bulge and LMC/SMC by the OGLE-III survey, only about 200 stars have been reported in all field RR Lyrae stars studies to date; the sample presented here nearly doubles the number of field RR Lyrae stars displaying the Blazhko effect. With time-resolved photometry expected from LSST, a similar analysis will be performed for RR Lyrae stars in the southern sky and we anticipate a higher fraction of discovered Blazhko stars due to better sampling and superior photometric quality.

Key words. Variable stars — RR Lyrae stars — Blazhko Effect

1. Introduction

RR Lyrae stars are pulsating variable stars with periods in the range of 3–30 hours and large amplitudes that increase towards blue optical bands (e.g., in the SDSS g band from 0.2 mag to 1.5 mag; Sesar et al. 2010). For comprehensive reviews of RR Lyrae stars, we refer the reader to Smith (1995) and Catelan (2009).

RR Lyrae stars often exhibit amplitude and phase modulation, or the so-called Blazhko effect[1] (hereafter, "Blazhko stars"). For examples of well-sampled observed light curves showing the Blazhko effect, see, e.g., Kepler data shown in Figures 1 and 2 from Benkő et al. (2010). The Blazhko effect has been known for a long time (Blažko 1907), but its detailed observational properties and theoretical explanation of its causes remain elusive (Kolenberg 2008; Kovács 2009; Szabó 2014). Various proposed models for the Blazhko effect, and principal reasons why they fail to explain observations, are summarized in Kovacs (2016).

A part of the reason for the incomplete observational description of the Blazhko effect is difficulties in discovering a large number of Blazhko stars due to temporal baselines that are too short and insufficient number of observations per object (Kovacs 2016; Hernitschek & Stassun 2022). With the advent of modern sky surveys, several studies reported large increases in the number of known Blazhko stars, starting with a sample of about 700 Blazhko stars discovered by the MACHO survey towards the LMC (Alcock et al. 2003) and about 500 Blazhko stars discovered by the OGLE-II survey towards the Galactic bulge (Mizerski 2003). Most recently, about 4,000 Blazhko stars were discovered in the LMC and SMC (Soszyński et al. 2009, 2010), and an additional ~3,500 stars were discovered in the Galactic bulge (Soszyński et al. 2011; Prudil & Skarka 2017), both by the OGLE-III survey. Nevertheless, discovering the Blazhko effect in field RR Lyrae stars that are spread over the entire sky remains a much harder problem: only about 200 Blazhko stars in total from all the studies of field RR Lyrae stars have been reported so far (see Table 1 in Kovacs 2016).

Here, we report the results of a search for the Blazhko effect in a sample of ~3,000 field RR Lyrae stars with LINEAR and ZTF light curve data. A preliminary subsample of about ~530 stars was selected using various light curve statistics, and then 228 stars were confirmed visually as displaying the Blazhko effect. This new sample greatly increases the number of known field RR Lyrae stars that exhibit the Blazhko effect. In §2 and §3 we describe our datasets and analysis methodology, and in §4 we present our analysis results. Our main results are summarized and discussed in §5.

2. Data Description and Period Estimation

Analysis of field RR Lyrae stars requires a sensitive time-domain photometric survey over a large sky area. For our starting sample, we used ~3,000 field RR Lyrae stars with light curves obtained by the LINEAR asteroid survey. In order to study long-term changes in light curves, we also utilized light curves obtained by the ZTF survey which monitored the sky ~15 years after LINEAR. The combination of LINEAR and ZTF provided a unique opportunity to systematically search for the Blazhko effect in a large number of field RR Lyrae stars.

[1] The Blazhko effect was discovered by Lidiya Petrovna Tseraskaya and first reported by Sergey Blazhko.

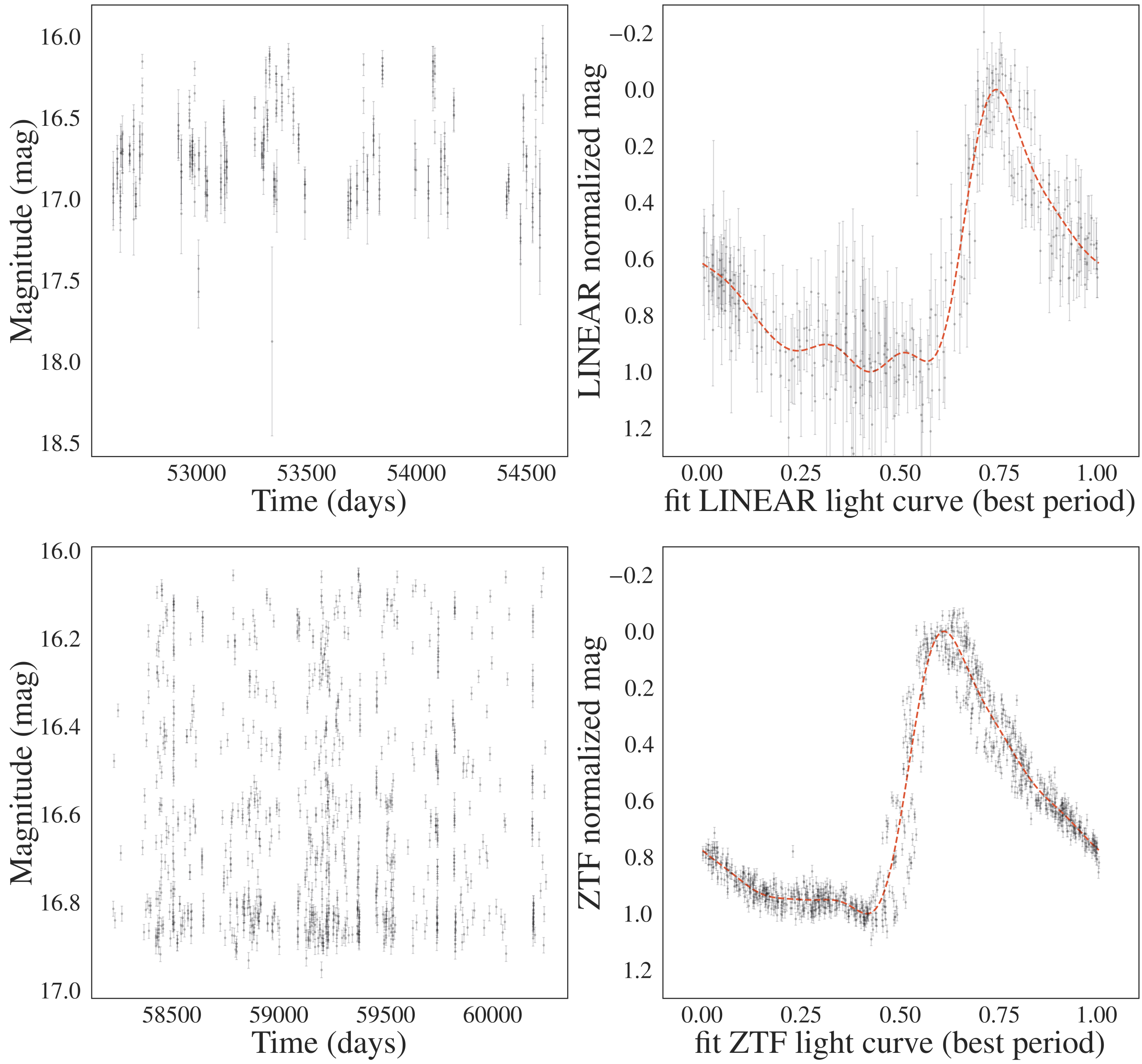

Fig. 1. An example of a Blazhko star (LINEARid = 136668) with LINEAR (top row) and ZTF (bottom row) light curves (left panels, data points with "error bars"), phased light curves normalized to the 0–1 range (right panels, data points with "error bars"), with their best-fit models shown by dashed lines. The best-fit period is determined for each dataset separately using 3 Fourier terms. The models shown in the right panels are evaluated with 6 Fourier terms.

We first describe each dataset in more detail, and then introduce our analysis methods. All our analysis code, written in Python, is available on GitHub[2].

2.1. LINEAR Dataset

The properties of the LINEAR asteroid survey and its photometric re-calibration based on SDSS data are discussed in Sesar et al. (2011). Briefly, the LINEAR survey covered about 10,000 deg^2 of the northern sky in white light (no filters were used, see Figure 1 in Sesar et al. 2011), with photometric errors ranging from ∼0.03 mag at an equivalent SDSS magnitude of $r = 15$ to 0.20 mag at $r \sim 18$. Light curves used in this work include, on average, 270 data points collected between December 2002 and September 2008.

A sample of 7,010 periodic variable stars with $r < 17$ discovered in LINEAR data were robustly classified by Palaversa et al. (2013), including about ∼3,000 field RR Lyrae stars of both ab and c type, detected to distances of about 30 kpc (Sesar et al. 2013). The sample used in this work contains 2196 ab-type and 745 c-type RR Lyrae, selected using classification labels and the *gi* color index from Palaversa et al. (2013). The LINEAR light curves, augmented with IDs, equatorial coordinates, and other data, were accessed using the astroML Python module[3] (VanderPlas et al. 2012).

[2] `https://github.com/emadonev/var_stars`

[3] For an example of light curves, see `https://www.astroml.org/book_figures/chapter10/fig_LINEAR_LS.html`

2.2. ZTF Dataset

The Zwicky Transient Factory (ZTF) is an optical time-domain survey that uses the Palomar 48-inch Schmidt telescope and a camera with 47 deg^2 field of view (Bellm et al. 2019). The dataset analyzed here was obtained with SDSS-like g, r, and i band filters. Light curves for objects in common with the LINEAR RR Lyrae sample typically have smaller random photometric errors than LINEAR light curves because ZTF data are deeper (compared to LINEAR, ZTF data have about 2-3 magnitudes fainter 5σ depth). ZTF data used in this work were collected between February 2018 and December 2023, on average about 15 years after obtaining LINEAR data.

The ZTF dataset for this project was created by selecting ZTF IDs with matching equatorial coordinates to a corresponding LINEAR ID of an RR Lyrae star. This process used the *ztfquery* function, which searched the coordinates in the ZTF database within 3 arcsec from the LINEAR position. The resulting sample consisted of 2857 RR Lyrae stars with both LINEAR and ZTF data. The fractions of RRab and RRc type RR Lyrae in this sample, 71% RRab and 29% RRc type, are consistent with results from other surveys (e.g., Sesar et al. 2010).

2.3. Period Estimation

The first step of our analysis is estimating best-fit periods, separately for LINEAR and ZTF datasets. We used the Lomb-Scargle method (Vanderplas 2015) as implemented in *astropy* (Astropy Collaboration et al. 2018). The period estimation used 3 Fourier components and a two-step process: an initial best-fit frequency was determined using the *autopower* frequency grid option and then the power spectrum was recomputed around the initial frequency using an order of magnitude smaller frequency step. In case of ZTF, we estimated period separately for each available passband and adopted their median value. Once the best-fit period was determined, a best-fit model for the phased light curve was computed using 6 Fourier components. Fig 1 shows an example of a star with LINEAR and ZTF light curves, phased light curves, and their best-fit models.

We found excellent agreement between the best-fit periods estimated separately from LINEAR and ZTF light curves. The median of their ratio is unity within 2×10^{-6} and the robust standard deviation of their ratio is 2×10^{-5}. With a median sample period of 0.56 days, the implied scatter of period difference is about 1.0 sec.

Given on average about 15 years between LINEAR and ZTF data sets, and a typical period of 0.56 days, this time difference corresponds to about 10,000 oscillations. With a fractional period uncertainty of 2×10^{-5}, LINEAR data can predict the phase of ZTF light curve with an uncertainty of 0.2. Therefore, for a robust detection of light curve phase modulation, each data set must be analyzed separately. On the other hand, amplitude modulation can be detected on time scales as long as 15 years, as discussed in the following section.

3. Analysis Methodology: Searching for the Blazhko Effect

Given the two sets of light curves from LINEAR and ZTF, we searched for amplitude and phase modulation, either during the 5-6 years of data taking by each survey, or during the average span of 15 years between the two surveys. Starting with a sample of 2857 RR Lyrae stars, we pre-selected a smaller sample

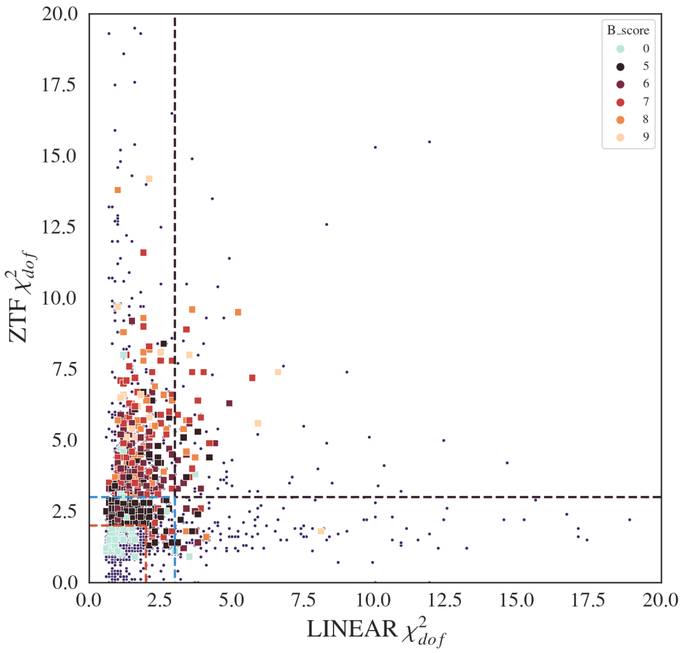

Fig. 2. A selection diagram constructed with the two sets of robust χ^2_{dof} values, for LINEAR and ZTF data sets, where the dark blue symbols represents all RR Lyrae stars, while the squares represent all the Blazhko candidate stars. The varying shades of the squares represent the number of points they scored during the selection algorithm, indicated by the legend. The horizontal and vertical dashed lines mark Blazhko candidate selection boundaries (see text).

that was inspected visually (see below for details). We also required at least 150 LINEAR data points and 150 ZTF data points (for the selected band from which we calculated the period) in analyzed light curves. We used two pre-selection methods that are sensitive to different types of light curve modulation: direct light curve analysis and periodogram analysis, as follows.

3.1. Direct Light Curve Analysis

Given statistically correct period, amplitude and light curve shape estimates, as well as data being consistent with reported (presumably Gaussian) uncertainty estimates, the χ^2 per degree of freedom gives a quantitative assessment of the *"goodness of fit"*,

$$\chi^2_{dof} = \frac{1}{N_{dof}} \sum \frac{(d_i - m_i)^2}{\sigma_i^2}. \quad (1)$$

Here, d_i are measured light curve data values at times t_i, and with associated uncertainties σ_i, m_i are best-fit models at times t_i, and N_{dof} is the number of degrees of freedom, essentially the number of data points. In the absence of any light curve modulation, the expected value of χ^2_{dof} is unity, with a standard deviation of $\sqrt(2/N_{dof}$. If $\chi^2_{dof} - 1$ is many times larger than $\sqrt(2/N_{dof}$, it is unlikely that data d_i were generated by the assumed (unchanging) model m_i. Of course, χ^2_{dof} can also be large due to underestimated measurement uncertainties σ_i, or to occasional non-Gaussian measurement error (the so-called outliers).

Therefore, to search for signatures of the Blazhko effect, manifested through statistically unlikely large values of χ^2_{dof}, we computed χ^2_{dof} separately for LINEAR and ZTF data (see Figure 2). Using the two sets of χ^2_{dof} values, we algorithmically pre-

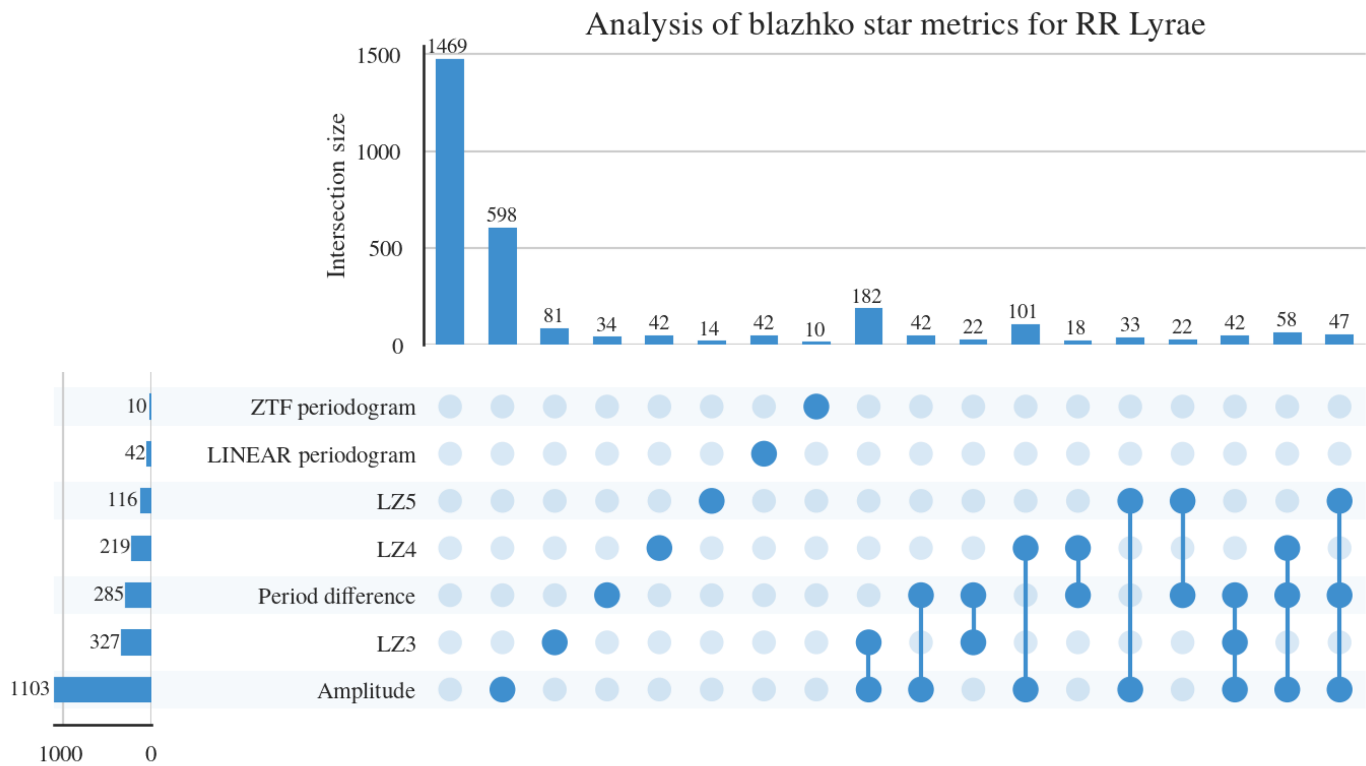

Fig. 3. The figure shows selection criteria and the resulting numbers of pre-selected Blazhko star candidates for each criterion and their combinations. The dots represent each case a star can occupy, where every solid dot is a specific criterion that is satisfied. Connections between solid dots represent stars which satisfy multiple criteria. Each dot combination has its own count, represented by the horizontal countplot. The vertical countplot shows the total number of stars that satisfy one criteria (union of all cases).

selected a sample of candidate Blazhko stars for further visual analysis of their light curves. The visual analysis is needed to confirm the expected Blazhko behavior in observed light curves, as well as to identify cases of data problems, such as photometric outliers.

We used a simple scoring algorithm, optimized through trial and error, illustrated in Fig. 2 with dashed lines signifying χ^2_{dof} boundaries. The algorithm used area boundaries for χ^2_{dof} values (χ^2_L is the χ^2_{dof} value for LINEAR, while χ^2_Z is analogous for ZTF data.)

The *3-point area* includes ranges of:

1. $\chi^2_L > 2.0$ and $\chi^2_L < 3.0$ and $\chi^2_Z > 2.0$ and $\chi^2_Z < 3.0$,
2. $\chi^2_L > 2.0$ and $\chi^2_L < 3.0$ and $\chi^2_Z < 3.0$,
3. $\chi^2_Z > 2.0$ and $\chi^2_Z < 3.0$ and $\chi^2_L < 3.0$.

The *4-point area* includes ranges of:

1. $\chi^2_L > 3.0$ and $\chi^2_L < 5.0$ and $\chi^2_Z < 3.0$
2. $\chi^2_L < 3.0$ and $\chi^2_Z > 3.0$ and $\chi^2_Z < 5.0$

The *5-point area* includes ranges of:

1. $\chi^2_L > 5.0$ and $\chi^2_Z > 5.0$
2. $\chi^2_L > 3.0$ and $\chi^2_L < 5.0$ and $\chi^2_Z > 3.0$ and $\chi^2_Z < 5.0$
3. $\chi^2_L > 5.0$ and $\chi^2_Z < 5.0$
4. $\chi^2_Z > 5.0$ and $\chi^2_L < 5.0$

In addition, we also considered normalized period differences (dP) and amplitude differences (dA) and assigned: 1 points for $0.00002 < dP < 0.00005$ and 2 points for $dP > 0.00005$; 1 point for $0.05 < dA < 0.15$ and 2 points for $dA > 0.15$. A star could score a maximum of 9 points, and a minimum of 5 points was required for further visual analysis.

The sample pre-selected using this method includes 531 stars. For most selected stars, the χ^2_{dof} values were larger for the ZTF data because the ZTF photometric uncertainties are smaller than for the LINEAR data set. Fig. 3 summarizes the selection criteria and the resulting numbers of selected stars for each criterion and their combinations.

3.2. Periodogram Analysis

When light curve modulation is due to double-mode oscillation with two similar oscillation frequencies (periods), it is possible to recognize its signature in the periodogram computed as part of the Lomb-Scargle analysis. Depending on various details, such as data sampling and the exact values of periods, amplitudes, this method may be more efficient than direct light curve analysis (Skarka et al. 2020).

A sum of two *sine* functions with same amplitudes and with frequencies f_1 and f_2 can be rewritten using trigonometric equalities as

$$y(t) = 2\cos(2\pi\frac{f_1 - f_2}{2}t)\,\sin(2\pi\frac{f_1 + f_2}{2}t). \quad (2)$$

We can define

$$f_o = \frac{f_1 + f_2}{2}, \quad (3)$$

and

$$\Delta f = |\frac{f_1 - f_2}{2}|, \quad (4)$$

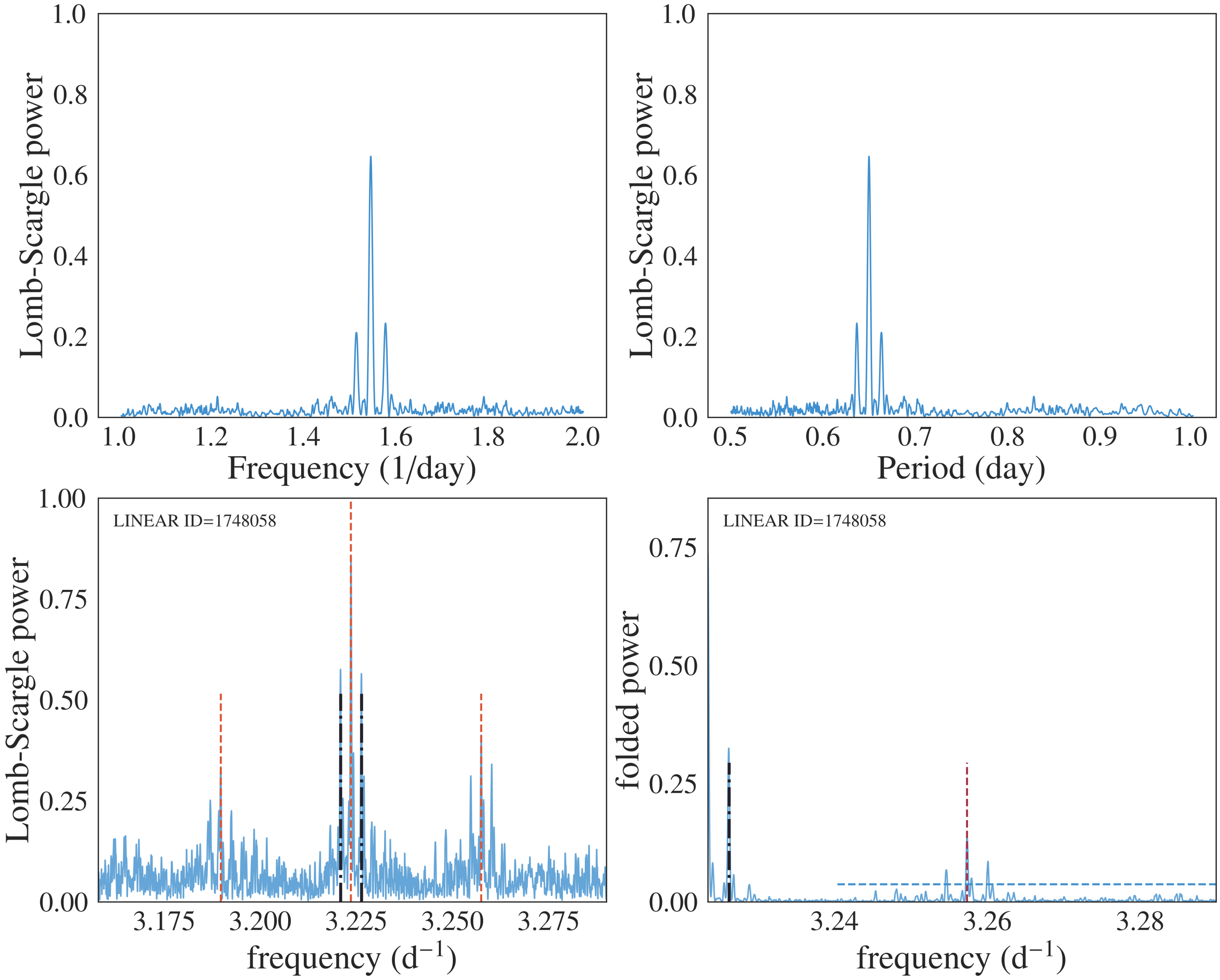

Fig. 4. The top two panels show a simulated periodogram for a sum of two *sine* functions with similar frequencies f_1 and f_2 – the central peak corresponds to their mean (see eqs. 3 and 4). The bottom left panel shows a periodogram for an observed LINEAR light curve for ID = 1748058, and the bottom right panel shows its folded version (around the main frequency f_o = 3.223 d^{-1}). In the bottom left panel, the three vertical dashed lines show the three frequencies identified by the algorithm described in text, and the two dot-dashed lines mark yearly aliases around the main frequency f_o, at frequencies $f_o \pm 0.034$ d^{-1}. The two vertical lines in the bottom right panel have the same meaning, and the horizontal dashed line shows the noise level multiplied by 5.

with $\Delta f << f_o$ when f_1 and f_2 are similar. The fact that Δf is much smaller than f_o means that the period of the *cos* term is much larger than the period of the basic oscillation (f_o). In other words, the *cos* term acts as a slow amplitude modulation of the basic oscillation. When the amplitudes of two *sine* functions are not equal, the results are more complicated but the basic conclusion about amplitude modulation remains. When the power spectrum of $y(t)$ is constructed, it will show 3 peaks: the main peak at f_o and two more peaks at frequencies $f_o \pm \Delta f$. We used this fact to construct an algorithm for automated searching for the evidence of amplitude modulation. Fig 4 compares the theoretical periodogram produced by interference beats with our algorithm's periodogram, signifying that local Blazhko peaks are present in real data.

After the strongest peak in the Lomb-Scargle periodogram is found at frequency f_o, we search for two equally distant local peaks at frequencies f_- and f_+, with $f_- < f_0 < f_+$. The side-band peaks can be highly asymmetric Alcock et al. (2003) and observed periodograms can sometimes be much more complex Szczygieł & Fabrycky (2007). We fold the periodogram through the main peak at f_o, multiply the two branches and then search for the strongest peaks in the resulting folded periodogram that is statistically more significant than the background noise. The background noise is computed as the scatter of the folded periodogram estimated from the interquartile range. We require a "signal-to-noise" ratio of at least 5, as well as the peak strength of at least 0.05 for ZTF, while 0.10 for LINEAR data. If such a peak is found, and it doesn't correspond to yearly alias, we select the star as a candidate Blazhko star and compute its Blazhko period as

$$P_{BL} = |f_{-,+} - f_0|^{-1},$$

where $f_{-,+}$ means the Blazhko sideband frequency with a higher amplitude is chosen.

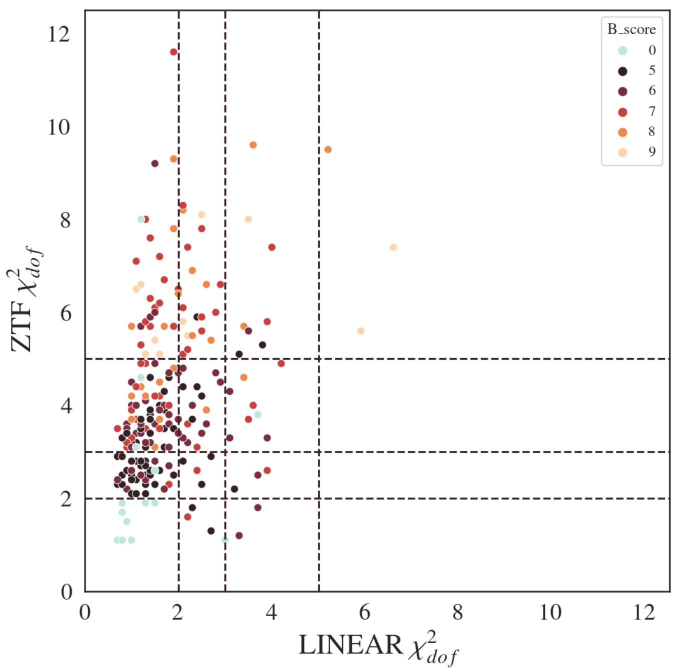

Fig. 5. The figure shows in which χ^2_{dof} area Blazhko stars are. Each dot is colored a different shade of red based on its score during selection, while blue dots are stars selected via periodogram.

The observed Blazhko periods range from 3 to 3,000 days, and Blazhko amplitudes range from 0.01 mag to about 0.3 mag (Szczygieł & Fabrycky 2007). In this work, we selected a smaller Blazhko range due to the limitations of our data: 30–325 days. With this additional constraint, we selected 52 candidate Blazhko stars. Fig 4 shows an example where two very prominent peaks were identified in the LINEAR periodogram.

3.2.1. Visual Confirmation

The sample pre-selected for visual analysis includes 531 RR Lyrae stars (479 + 52), or 18.1% of the starting LINEAR-ZTF sample. Visual analysis included the following standard steps (e.g., Jurcsik et al. 2009; Prudil & Skarka 2017):

1. The shape of the phased light curves and scatter of data points around the best-fit model were examined for signatures of anomalous behavior indicative of the Blazhko effect. Fig. 6 shows an example of such behavior where the ZTF data and fit show multiple coherent data point sequences offset from the best-fit mean model.
2. Full light curves were inspected for their repeatability between observing seasons (Fig. 7). This step was sensitive to amplitude modulations with periods of the order a year or longer.
3. The phased light curves normalized to unit amplitude were inspected for their repeatability between observing seasons. This step was sensitive to phase modulations of a few percent or larger on time scales of the order a year or longer. Fig. 8 shows an example of a Blazhko star where season-to-season phase (and amplitude) modulations are seen in both the LINEAR data and (especially) the ZTF data.

After visually analyzing the starting sample of 531 Blazhko candidates, we visually confirmed expected Blazhko behavior for 228 stars (214 out of 479 and 14 out of 52). LINEAR IDs and other characteristics for confirmed Blazhko stars are listed in Table 1 (Appendix A). Statistical properties of the selected sample of Blazhko stars are discussed in detail in the next section.

4. Results

Starting with a sample of 2857 field RR Lyrae stars with both LINEAR and ZTF data, we found 228 stars exhibiting convincing Blazhko effect. Out of these 228, 14 were selected via periodogram, and 214 via the scoring algorithm.

From Fig. 5 we can see that most Blazhko stars selected via periodogram have very low χ^2_{dof} values for both LINEAR and ZTF data. Meanwhile, Blazhko stars selected via the scoring algorithm generally have low χ^2_{dof} LINEAR scores, with an average of 1.78, and higher χ^2_{dof} ZTF values, with an average of 4.09. Most Blazhko stars are part of the 4-point χ^2_{dof} range (94 stars), with 66 stars in the 5-point range and 54 in the 3-point range. In accordance with this, the average Blazhko candidate score is 5.90. Based on the light curve type, 78.95 % of stars are RRab type, and 21.05 % are RRc type stars. Ratio of RRab to RRc stars is in accordance with other works.

During visual analysis, we noticed that many Blazhko stars exhibited convincing Blazhko effect either in LINEAR or in ZTF data, with few examples of the effect in both datasets. Also, the modulation in light curves isn't constant for most stars, rather it varies throughout the observing season. In the following discussion we discuss how to utilize this finding.

5. Discussion and Conclusions

The reported incidence rates for the Blazhko effect range from 5% (Szczygieł & Fabrycky 2007) to 60% (Szabó et al. 2014). For a relatively small sample of 151 stars with Kepler data, a claim has been made that essentially every RR Lyrae star exhibits modulated light curve (Kovacs 2018). The difference in Blazhko incidence rates for the two most extensive samples, obtained by the OGLE-III survey for the Large Magellanic Cloud (LMC, 20% out of 17,693 stars; Soszyński et al. 2009). Moreover, the Galactic bulge (30% out of 11,756 stars; Soszyński et al. 2011) indicates a possible variation of the Blazhko incidence rate with underlying stellar population properties. In this work, 7.75% of the original RR Lyrae dataset are Blazhko stars. Since our sample size is considerable, we conclude that the incidence rate of Blazhko stars in our work is representative and aligns with other works. We theorize that the difference in incidence rates occurs due to varying data precision, the temporal baseline length, and differences in visual or algorithmic analysis. We also conclude that our algorithm's success rate in finding 228 out of 531 potential Blazhko stars is 43% . This high number indicates that the algorithm is quite successful and can be used and refined further for efficient Blazhko star selection.

For future research, we would like to explore the final finding and find a connection or a factor that might give rise to a mechanism that explains the Blazhko effect. Due to the significant time difference between LINEAR and ZTF observing times (around 15 years difference), stars where the effect is found in both datasets might prove very interesting as they show the Blazhko effect to be long lasting and present for long periods of time in relation to the short period of RR Lyrae stars. Based on the final finding, we confirm that the light curve modulation can be unstable, as discussed by Jurcsik et al. (2009) The project is an excellent example of automatizing the search for Blazhko stars. It can further be improved by training a neural network to

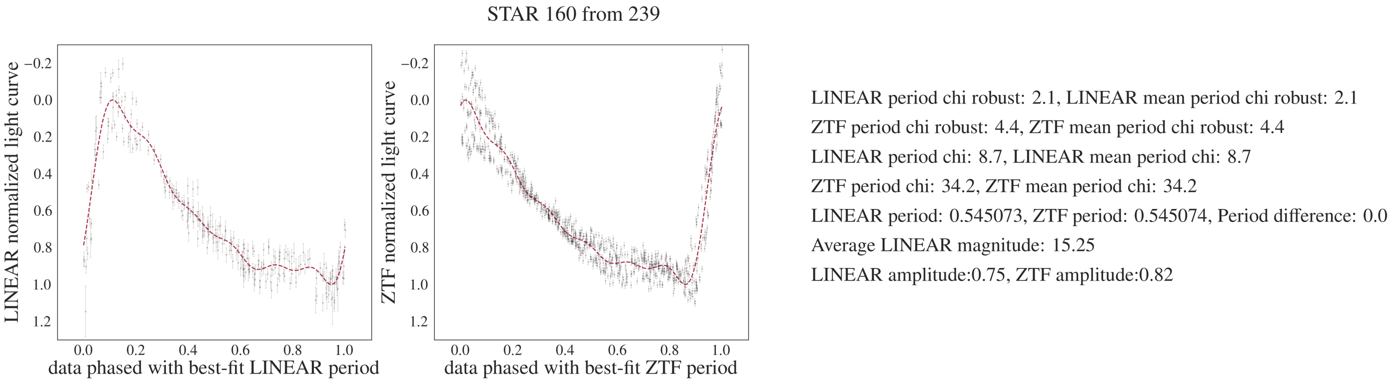

Fig. 6. An illustration of visual analysis of phased light curves for the selected Blazhko candidates. The left panel shows LINEAR data and the right panel shows ZTF data (symbols with "error bars") for star with LINEARid = 10030349. The dashed lines are best-fit models. The numbers listed on the right side were added to aid visual analysis. Note multiple coherent data point sequences offset from the best-fit mean model in the right panel.

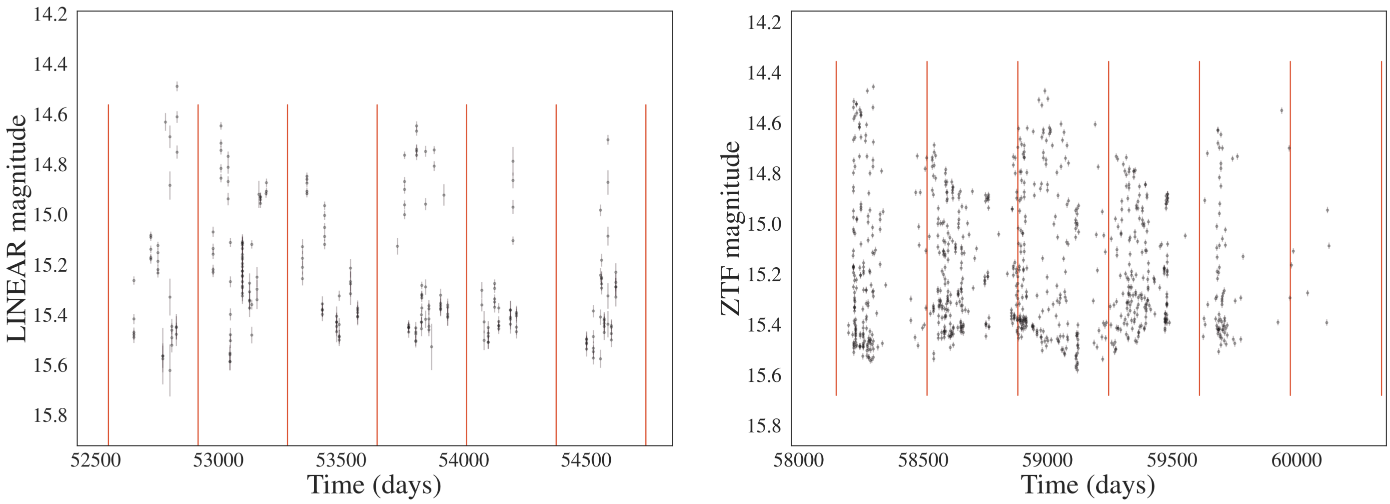

Fig. 7. An illustration of visual analysis of full light curves for the selected Blazhko candidates with emphasis on their repeatability between observing seasons, marked with vertical lines (left: LINEAR data; right: ZTF data). Data shown are for star with LINEARid = 10030349.

replace visual analysis, and our current algorithms can be improved with other models. This work can provide a base for finding more Blazhko stars for the future Vera Rubin observatory. The Legacy Survey of Space and Time (LSST; Ivezić et al. 2019) will be an excellent survey for studying Blazhko effect (Hernitschek & Stassun 2022) because it will have both a long temporal baseline (10 years) and a large number of observations per object (nominally 825; LSST Science Requirements Document[4]).

A prominent issue in this work is a short temporal baseline which results in few datapoints, limiting our ability to find small changes or modulations in the data. With time-resolved photometry expected from LSST, a similar analysis will be performed for RR Lyrae stars in the southern sky and we anticipate a higher fraction of discovered Blazhko stars due to better sampling and superior photometric quality, since the incidence rate of the Blazhko effect increases with sensitivity to small-amplitude modulation, and thus with photometric data quality (Jurcsik et al. 2009).

(Skarka et al. 2020) classify Blazhko stars in 6 classes using the morphology of their amplitude modulation (though we note that the most dominant class includes 90% of the sample). They find bimodal distribution of Blazko periods, with two components centered on 48 d and 186 d.

LINEAR and ZTF data used here do not have as many data points as OGLE-III used by them (comment earlier, in Introduction? also Kepler is great, (Benkő et al. 2010)).

From Jurcsik et al. (2009): A sample of 30 RRab stars was extensively observed, and light-curve modulation was detected in 14 cases. The 47 per cent occurrence rate of the modulation is much larger than any previous estimate.

Acknowledgements. We thank Mathew Graham for providing *ztfquery* code example to us. Ž.I. acknowledges funding by the Fulbright Foundation and thanks the Ruđer Bošković Institute (Zagreb, Croatia) for hospitality. Based on observations obtained with the Samuel Oschin Telescope 48-inch and the 60-inch Telescope at the Palomar Observatory as part of the Zwicky Transient Facility project. ZTF is supported by the National Science Foundation under Grants No. AST-1440341 and AST-2034437 and a collaboration including current partners Caltech, IPAC, the Weizmann Institute of Science, the Oskar Klein Center at Stockholm University, the University of Maryland, Deutsches Elektronen-Synchrotron and Humboldt University, the TANGO Consortium of Taiwan, the University of Wisconsin at Milwaukee, Trinity College Dublin, Lawrence Livermore National Laboratories, IN2P3, University of Warwick, Ruhr University Bochum, Northwestern University and former partners the University of Washington, Los Alamos National Laboratories, and Lawrence Berkeley National Laboratories. Operations are conducted by COO, IPAC, and UW. The LINEAR program is funded by the National Aeronautics and Space Administration at MIT Lincoln Laboratory under Air Force Contract FA8721-05-C-0002. Opinions, in-

[4] Available as ls.st/srd

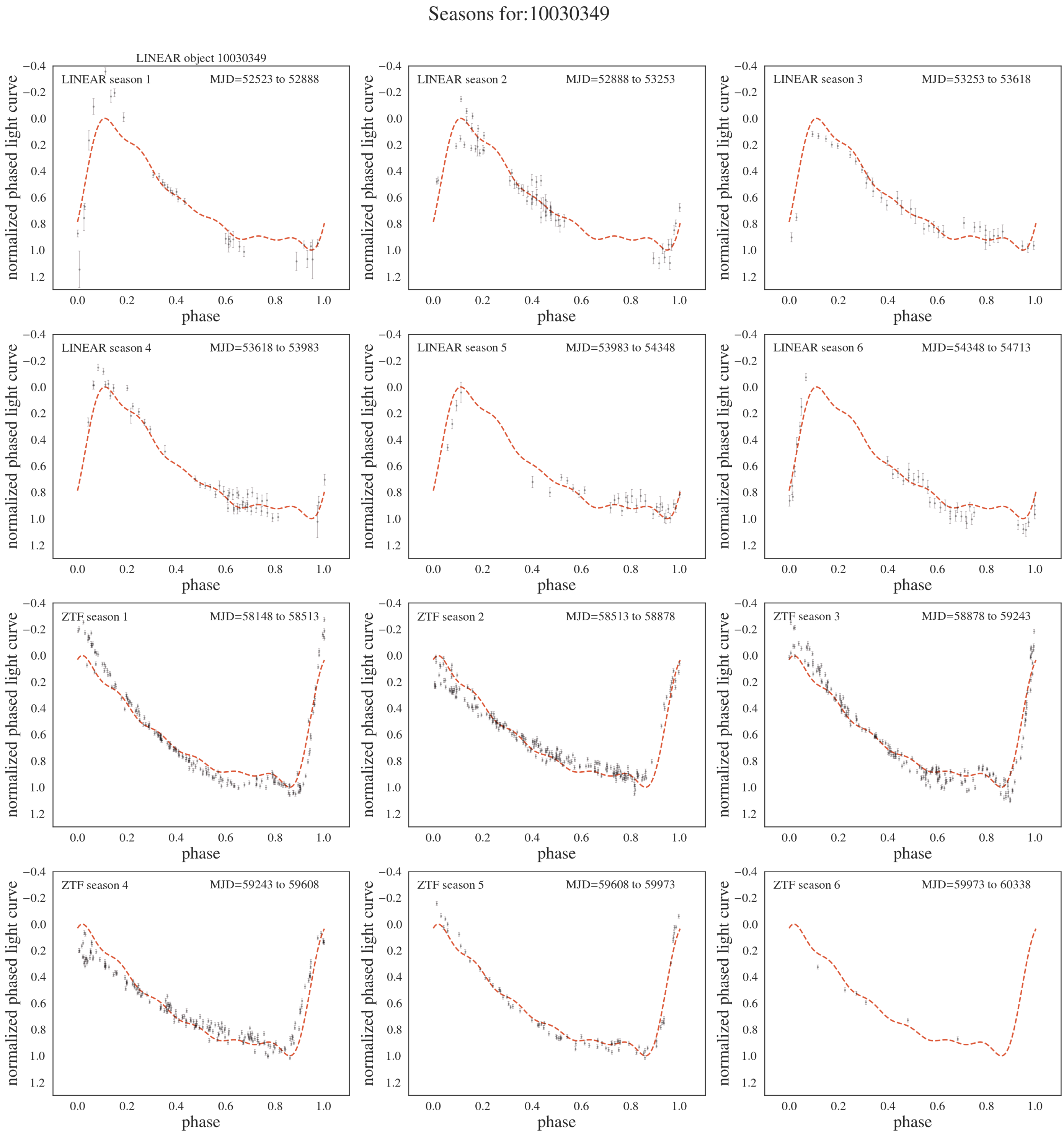

Fig. 8. The phased light curves normalized to unit amplitude are shown for single observing seasons and compared to the mean best-fit models (top six panels: LINEAR data; bottom six panels: ZTF data). Data shown are for star with LINEARid = 10030349. Season-to-season phase and amplitude modulations are seen in both the LINEAR and the ZTF data.

terpretations, conclusions and recommendations are those of the authors and are not necessarily endorsed by the United States Government.

References

Alcock, C., Alves, D. R., Becker, A., et al. 2003, ApJ, 598, 597

Astropy Collaboration, Price-Whelan, A. M., Sipőcz, B. M., et al. 2018, AJ, 156, 123

Bellm, E. C., Kulkarni, S. R., Graham, M. J., et al. 2019, PASP, 131, 018002

Benkő, J. M., Kolenberg, K., Szabó, R., et al. 2010, MNRAS, 409, 1585

Blažko, S. 1907, Astronomische Nachrichten, 175, 325

Catelan, M. 2009, Ap&SS, 320, 261

Hernitschek, N. & Stassun, K. G. 2022, ApJS, 258, 4

Ivezić, Ž., Kahn, S. M., Tyson, J. A., et al. 2019, ApJ, 873, 111

Jurcsik, J., Sódor, Á., Szeidl, B., et al. 2009, MNRAS, 400, 1006
Kolenberg, K. 2008, in Journal of Physics Conference Series, Vol. 118, Journal of Physics Conference Series (IOP), 012060
Kovács, G. 2009, in American Institute of Physics Conference Series, Vol. 1170, Stellar Pulsation: Challenges for Theory and Observation, ed. J. A. Guzik & P. A. Bradley, 261–272
Kovacs, G. 2016, Commmunications of the Konkoly Observatory Hungary, 105, 61
Kovacs, G. 2018, A&A, 614, L4
Mizerski, T. 2003, Acta Astron., 53, 307
Palaversa, L., Ivezić, Ž., Eyer, L., et al. 2013, AJ, 146, 101
Prudil, Z. & Skarka, M. 2017, MNRAS, 466, 2602
Sesar, B., Ivezić, Ž., Grammer, S. H., et al. 2010, ApJ, 708, 717
Sesar, B., Ivezić, Ž., Stuart, J. S., et al. 2013, AJ, 146, 21
Sesar, B., Stuart, J. S., Ivezić, Ž., et al. 2011, AJ, 142, 190
Skarka, M., Prudil, Z., & Jurcsik, J. 2020, MNRAS, 494, 1237
Smith, H. A. 1995, Cambridge Astrophysics Series, 27
Soszyński, I., Dziembowski, W. A., Udalski, A., et al. 2011, Acta Astron., 61, 1
Soszyński, I., Udalski, A., Szymański, M. K., et al. 2010, Acta Astron., 60, 165
Soszyński, I., Udalski, A., Szymański, M. K., et al. 2009, Acta Astron., 59, 1
Szabó, R. 2014, in IAU Symposium, Vol. 301, Precision Asteroseismology, ed. J. A. Guzik, W. J. Chaplin, G. Handler, & A. Pigulski, 241–248
Szabó, R., Benkő, J. M., Paparó, M., et al. 2014, A&A, 570, A100
Szczygieł, D. M. & Fabrycky, D. C. 2007, MNRAS, 377, 1263
Vanderplas, J. 2015, gatspy: General tools for Astronomical Time Series in Python
VanderPlas, J., Connolly, A. J., Ivezic, Z., & Gray, A. 2012, in Proceedings of Conference on Intelligent Data Understanding (CIDU, 47–54

Appendix A: Full table of results

Here we present the first 50 confirmed Blazhko stars with their LINEAR IDs, equatorial coordinates, and calculated periods and χ^2 values.

LINEAR ID	Plinear	Pztf	N_L	N_Z	L_chi2r	Z_chi2r	L_chi2	Z_chi2	Lampl	Zampl	Ampl_diff	BpeakL	BpeakZ	BperiodL	BperiodZ	LCtype	Periodogram_f	B_score
158779	0.609207	0.609189	293	616	1.6	3.9	3.7	34.2	0.47	0.68	0.21	1.6443	1.6444	352.7337	350.2627	1	-	7
263541	0.558218	0.558221	270	503	2.9	6.6	15.8	110.4	0.64	0.82	0.18	1.8621	1.8025	14.1513	89.9685	1	-	7
393084	0.530027	0.530033	493	372	1.1	3.2	1.6	19.2	0.96	1.31	0.35	1.9447	1.8896	17.2369	347.2222	1	-	6
810169	0.465185	0.465212	289	743	2.1	2.8	6.0	15.1	0.77	0.75	0.02	2.2232	2.2230	13.6017	13.6082	1	-	5
924301	0.507503	0.507440	418	189	1.9	9.3	13.8	162.9	0.87	0.79	0.08	2.0043	1.9763	29.5072	178.4121	1	-	8
970326	0.592233	0.592231	275	552	1.1	2.1	1.9	7.7	0.51	0.75	0.24	1.7563	1.6992	14.7656	93.2836	1	-	5
999528	0.658401	0.658407	564	213	1.2	2.7	1.8	21.7	0.57	0.92	0.35	1.5527	1.5510	29.5247	31.0366	1	-	5
1005497	0.653607	0.653605	607	192	1.1	2.1	2.1	12.4	0.60	0.83	0.23	1.5639	1.5481	29.4638	55.1116	1	-	5
1092244	0.649496	0.649558	590	326	1.2	3.6	2.3	32.1	0.72	0.58	0.14	1.5735	1.5640	29.5421	40.8330	1	-	7
1240665	0.632528	0.632522	468	311	3.0	1.1	25.2	1.6	0.33	0.33	0.00	1.6149	1.5865	29.4942	182.3154	1	Z	0
1244554	0.536875	0.536962	469	312	1.8	2.3	9.5	14.8	0.71	0.97	0.26	1.8966	1.9325	29.4638	14.2481	1	-	7
1271119	0.565270	0.565257	280	521	1.0	4.0	2.9	45.5	0.69	0.90	0.21	1.8366	1.7739	14.8060	208.3333	1	-	6
1332201	0.580711	0.580731	260	208	1.6	4.2	9.2	50.1	0.59	0.83	0.24	1.7559	1.7918	29.4942	14.3225	1	-	7
1390653	0.521867	0.521871	524	310	1.3	4.1	4.2	44.9	1.10	1.28	0.18	1.9502	2.0026	29.4291	11.5768	1	-	6
1448299	0.606912	0.606940	435	267	2.7	5.4	32.5	35.6	0.77	0.70	0.07	1.6816	1.6531	29.4551	180.9955	1	-	8
1539000	0.500288	0.500279	410	468	1.5	3.6	6.1	66.3	0.89	1.13	0.24	2.0021	2.0017	303.9514	355.8719	1	-	6
1593736	0.592628	0.592650	264	532	1.2	5.7	2.1	35.9	0.37	0.36	0.01	1.7584	1.6910	14.0795	272.4796	1	-	6
1748058	0.310237	0.310176	463	272	1.4	5.7	2.2	30.7	0.38	0.23	0.15	3.2572	3.2297	29.5203	173.3102	2	-	7
1790596	0.534498	0.534506	509	327	3.1	3.3	19.3	15.6	0.79	0.70	0.09	1.9046	1.8764	29.6868	182.1494	1	-	6
1882354	0.695061	0.695029	313	411	1.5	2.8	3.0	13.2	0.63	0.70	0.07	1.4909	1.4419	19.1516	326.2643	1	-	6
1936459	0.649248	0.649240	431	268	0.7	1.1	0.6	1.7	0.45	0.43	0.02	1.5741	1.5458	29.5203	181.8182	1	Z	0
2041979	0.653694	0.653639	276	1378	1.2	5.3	1.5	57.5	0.63	0.64	0.01	1.5944	1.5816	15.4607	19.3442	1	-	7
2050107	0.686454	0.686466	190	1388	3.9	3.3	16.4	22.3	0.78	0.64	0.14	1.4906	1.4633	29.5159	151.2859	1	-	6
2122319	0.359422	0.359424	519	199	2.1	6.1	7.2	36.6	0.38	0.55	0.17	2.8161	2.8926	29.5421	9.0645	2	-	7
2229607	0.575179	0.575211	290	731	1.2	4.4	2.7	38.3	0.55	0.81	0.26	1.8093	1.7433	14.1383	207.2539	1	-	8
2243683	0.579777	0.579803	531	262	3.1	4.3	22.0	36.0	0.52	0.56	0.04	1.7588	1.7303	29.4204	180.0180	1	-	6
2264042	0.655373	0.655391	391	299	1.6	4.0	6.5	57.4	0.74	0.76	0.02	1.5597	1.5313	29.5465	182.4818	1	-	5
2280940	0.562372	0.562374	310	735	1.1	3.2	1.4	17.5	0.84	1.01	0.17	1.8461	1.7847	14.7286	153.2567	1	-	6
2333087	0.551462	0.551424	560	202	3.5	8.0	29.8	90.2	0.72	0.88	0.16	1.8473	1.8304	29.5072	59.0842	1	-	9
2334384	0.555341	0.555333	443	204	2.0	6.5	10.5	84.7	0.63	0.88	0.25	1.8346	1.8353	29.5377	28.9394	1	-	7
2397296	0.488814	0.488836	522	196	1.2	6.6	3.2	78.9	0.65	1.01	0.36	2.0796	2.0672	29.5421	46.5224	1	-	9
2414841	0.559611	0.559592	522	305	1.7	5.7	5.6	62.8	0.69	1.09	0.40	1.8208	1.7920	29.5421	201.2072	1	-	8
2612592	0.571562	0.571543	270	1391	1.3	2.8	2.4	24.8	0.76	0.70	0.06	1.8173	1.7544	14.7787	208.5506	1	-	5
2683009	0.606278	0.606210	180	892	6.6	7.4	63.6	88.8	0.82	0.52	0.30	1.6833	1.6603	29.4942	93.7207	1	-	9
2851826	0.521838	0.521842	257	653	1.0	2.5	1.6	18.1	0.95	1.21	0.26	1.9595	1.9595	23.1642	23.1374	1	-	5
2889542	0.570913	0.570911	457	170	1.3	2.5	2.7	9.2	0.96	1.35	0.39	1.7855	1.8062	29.4855	18.3268	1	-	5
2892940	0.539855	0.539896	462	169	1.3	4.2	3.7	49.1	0.90	1.21	0.31	1.8862	1.9288	29.5290	13.0514	1	-	8
2936953	0.328746	0.328733	271	187	2.7	1.3	13.0	2.5	0.35	0.29	0.06	3.1123	3.0448	14.1995	356.5062	2	-	5
3140139	0.304590	0.304585	255	343	2.5	5.6	7.7	25.1	0.40	0.60	0.20	3.3529	3.4219	14.3338	7.2056	2	-	7
3183285	0.349653	0.349664	485	588	1.2	2.8	4.1	15.7	0.48	0.58	0.10	2.8939	2.8654	29.4768	181.8182	2	-	5
3196582	0.268017	0.268018	479	172	2.5	3.4	8.6	10.1	0.35	0.51	0.16	3.7650	3.8361	29.5203	9.5256	2	-	6
3196780	0.504148	0.504199	475	286	2.2	3.2	9.3	21.5	0.81	0.85	0.04	2.0029	1.9889	51.7331	181.6530	1	-	6
3219035	0.326746	0.326509	376	168	3.9	2.6	23.9	11.5	0.32	0.23	0.09	3.1287	3.0661	14.6692	294.1176	2	-	7
3463199	0.334718	0.334710	297	579	0.7	2.3	0.6	11.3	0.51	0.67	0.16	3.0584	2.9952	14.1153	133.2445	2	-	5
3491287	0.490986	0.490995	483	504	1.4	3.8	4.1	37.9	0.94	0.80	0.14	2.0537	2.0537	58.8408	58.8755	1	-	5
3589854	0.612893	0.612953	468	545	3.9	5.8	29.1	45.0	0.49	0.50	0.01	1.6656	1.6369	29.4031	184.6722	1	-	7